JMEPEG (2018) 27:2661–2667
https://doi.org/10.1007/s11665-018-3192-2

1059-9495/$19.00

Room Temperature Adsorptive Removal of Thiophene over Zinc Oxide-Based Adsorbents

Sohan Bir Singh and Mahuya De

(Submitted April 19, 2017; in revised form December 18, 2017; published online January 31, 2018)

This study investigated the room temperature adsorptive removal of thiophene over zinc oxide adsorbents in the presence of hydrogen. The bulk zinc oxide was prepared by precipitation method and calcined at different temperatures in the range of 300-550 °C. Supported zinc oxide was prepared by co-precipitation of 30 wt.% ZnO with alumina and calcined at 550 °C. Properties of the adsorbents were determined by various characterization techniques such as surface area and pore volume analysis, XRD, FESEM, EDX and TPR. The desulfurization process was carried out in a down-flow packed bed reactor at room temperature (30 °C). The BET surface area of bulk zinc oxide adsorbents decreased with the increase in calcination temperature from 300 to 550 °C. The surface area of bulk zinc oxide adsorbents was 30.5 and 14.6 m^2/g when calcined at 300 and 550 °C, respectively. The surface are of supported zinc oxide adsorbents was 177 m^2/g. The highest average pore size was obtained for bulk ZnO calcined at 550 °C (45 nm) compared to that calcined at 300 °C (42 nm) and supported ZnO (27 nm). The XRD peaks corresponded to the hexagonal structure of zinc oxide. The removal of thiophene was most significant for bulk ZnO calcined at 550 °C. The higher removal efficiency for this adsorbent in spite of lower surface area may be attributed to its higher percentage of larger pores and higher average pore size.

Keywords adsorption, desulfurization, thiophene, ZnO adsorbents

1. Introduction

The residue sulfur in transportation fuels is one of the major sources of air pollution. The stringent environment laws have necessitated the production of cleaner fuels (Ref 1). The worldwide allowed sulfur levels are different in different countries. In USA, the accepted sulfur level is 15 ppm for highway diesel since 2006 (Ref 2), while for Europe it is 10 ppm sulfur (Ref 3). Other developed countries such as Japan and Canada also follow similar regulations. In India, there is a two-tier system for fuel quality called Bharat Stage specifications (BS). The BS-IV grade diesel has been introduced in 13 major cities since April 2010, which requires a reduction of sulfur from the earlier 350 ppm level (BS-III) to 50 ppm (BS-IV) (Ref 4). Currently, sulfur is removed from diesel fuel by the conventional hydrodesulfurization process, in which the organic sulfur compounds are converted to H_2S at elevated temperature and pressure over suitable catalyst. The H_2S is removed later from the system by scrubbing with liquid (methanol) (Ref 5, 6). The major source of residue sulfur in diesel fuel is the sulfur compounds that are not removed by the conventional desulfurization processes. Many new approaches based on adsorption and oxidation of sulfur compounds have been recently proposed for removal of these non-reactive sulfur compounds, also known as refractory sulfur (Ref 7-10). The desulfurization by reactive adsorption is another effective method for deep removal of sulfur as it combines the advantages of the catalytic hydrodesulfurization and adsorption. The S-Zorb process of Conoco Philips Petroleum Co. based on reactive adsorption desulfurization at elevated temperature and low hydrogen pressure proved to be effective for the production of low-sulfur gasoline or diesel fuel (Ref 13). Various materials such as supported noble metals, transition metals, metal oxides, binary and ternary metal oxides, supported polymers were investigated for reactive adsorption (Ref 11-14). Metal containing zeolites or alumina supported adsorbents have been reported for the removal of sulfur compounds (Ref 15-17). The other types of reported desulfurization adsorbents included CaO, Fe_2O_3, MnO_2, ZnO, ZnO/TiO_2, ZnO/Fe_2O_3, ZnO/SiO_2, $CuO\text{-}Cr_2O_3$ (Ref 18). Zinc oxide-based desulfurization adsorbents were reported to be effective for H_2S removal, as the thermodynamics of reaction involving ZnO is more favorable compared to that of other desulfurization adsorbents (Ref 19). Thiophene was used as a typical test molecule for desulfurization studies because of its low reactivity (Ref 20).

For this study, bulk and supported zinc oxide-based adsorbents were developed to remove the sulfur compounds. The physical properties of bulk zinc oxides, such as surface area and pore size, were varied by calcining at different temperatures in the range of 300-550 °C. Alumina was used as the support to prepare supported zinc oxide adsorbent and was

This article is an invited paper selected from presentations at "ICETINN-2017, International Conference on Emerging Trends in Nanoscience and Nanotechnology," held March 16-18, 2017, in Majitar, Sikkim, India, and has been expanded from the original presentation.

Electronic supplementary material The online version of this article (https://doi.org/10.1007/s11665-018-3192-2) contains supplementary material, which is available to authorized users.

Sohan Bir Singh and **Mahuya De**, Department of Chemical Engineering, Indian Institute of Technology Guwahati, Guwahati, Assam 781039, India. Contact e-mails: sohanbir@iitg.ernet.in and mahuya@iitg.ernet.in.

prepared by co-precipitation method. The gas phase sulfur removal was studied in down-flow fixed bed reactor using thiophene as the source of sulfur in two different carrier gases, nitrogen and hydrogen, at room temperature and atmospheric pressure.

2. Experimental Work

2.1 Reagents and Chemicals

Zinc nitrate hexahydrate [$Zn(NO_3)_2.6H_2O$, 98% Aldrich] and aluminum nitrate [$Al(NO_3)_3{\cdot}9H_2O$, Merck] were used as precursors for preparation of zinc oxide and aluminum oxide, respectively. Ammonium hydroxide solution (NH_4OH, 30% Merck) and sodium hydroxide pallets (NaOH, 98% Rankem) were used as precipitating agents for the synthesis of aluminum hydroxide and zinc hydroxide, respectively. Thiophene (C_4H_4S, 99% Aldrich) was used as the source of sulfur, and toluene (C_7H_8, 99% Merck) was used as a solvent. All the chemicals were used in as-received conditions.

2.2 Preparation of Adsorbents

Figure 1(a) and (b) shows steps for preparation of bulk zinc oxide at different calcination temperatures and supported zinc oxide adsorbents, respectively. Preparation of bulk zinc oxide was carried out by precipitation from nitrate precursor solution using of 2 M NaOH solution. The pH was maintained at 10.5. After completion of precipitation, the mixture was aged at 75 °C for 6 h under stirred condition. The precipitate was filtered, washed and dried at 120 °C overnight. Finally, it was calcined at respective temperatures for 4 h. The prepared zinc oxides were referred in text as ZnO-X, where X denotes the calcination temperature of 300, 400 or 550 °C. The 30 wt.% zinc oxide supported on alumina was prepared by co-precipitation method. The loading was selected based on earlier study that showed 30 wt.% zinc oxide supported on alumina had the highest sulfur removal capacity compared to 20 and 40 wt.% loading (Supplementary Fig. S1). Zinc nitrate hexahydrate and aluminum nitrate were dissolved in required amount in deionised water separately. Zinc nitrate solution was added dropwise to the aluminum nitrate solution. The precipitation was carried out by 2 M NaOH solution at pH 10.5 as described earlier. The similar steps of aging, filtering, washing and drying were carried out. The calcination was done at 550 °C for 4 h, and supported zinc oxide adsorbent was referred in text as $30ZnO/Al_2O_3$-550.

2.3 Characterizations

Properties of the prepared samples were characterized by surface area and pore analyzer, x-ray diffraction (XRD), temperature-programmed reduction (TPR), field emission scanning electron microscopy (FESEM) and energy-dispersive x-ray (EDX) analysis. The surface area, pore volume and pore size distributions were determined by nitrogen physisorption at − 196 °C using a Beckman Coulter SA 3100 surface area analyzer. The samples were degassed at 150 °C in vacuum for 3 h prior to nitrogen adsorption–desorption measurements. The BET surface area was calculated using Brunauer–Emmett–Teller (BET) method, while total pore volume was determined at relative pressure (P_s/P_o) of 0.9814. The pore size distributions of samples were calculated using the Barrett–Joyner–Halenda (BJH) method. The XRD analysis of the samples was done using Bruker D8 advance diffractometer. Scanning was done in the range of 10-70° at rate of 0.5 s/step with an increment of 0.05. XRD patterns were obtained using Cu Kα radiation (λ = 0.154 nm). The x-ray source was operated at 45 kV and 40 mA. The morphology of the samples was determined using FESEM (Make: Zeiss; Model: 1430 VP). For FESEM analysis, the samples were dispersed in a solvent and deposited on aluminum foil which was then mounted on sample holder for gold coating. The EDX was used to confirm the presence of sulfur in the adsorbent after desulfurization test. TPR of the samples was carried out in Chemisorb 2720 (Make: Micromeritics). The adsorbent was pretreated at 150 °C for 1 h in the flow of nitrogen (30 ml/min). The temperature-programmed reduction was carried out in flow of 10% H_2-Ar gas mixture up to 700 °C using heating rate of 10 °C/min.

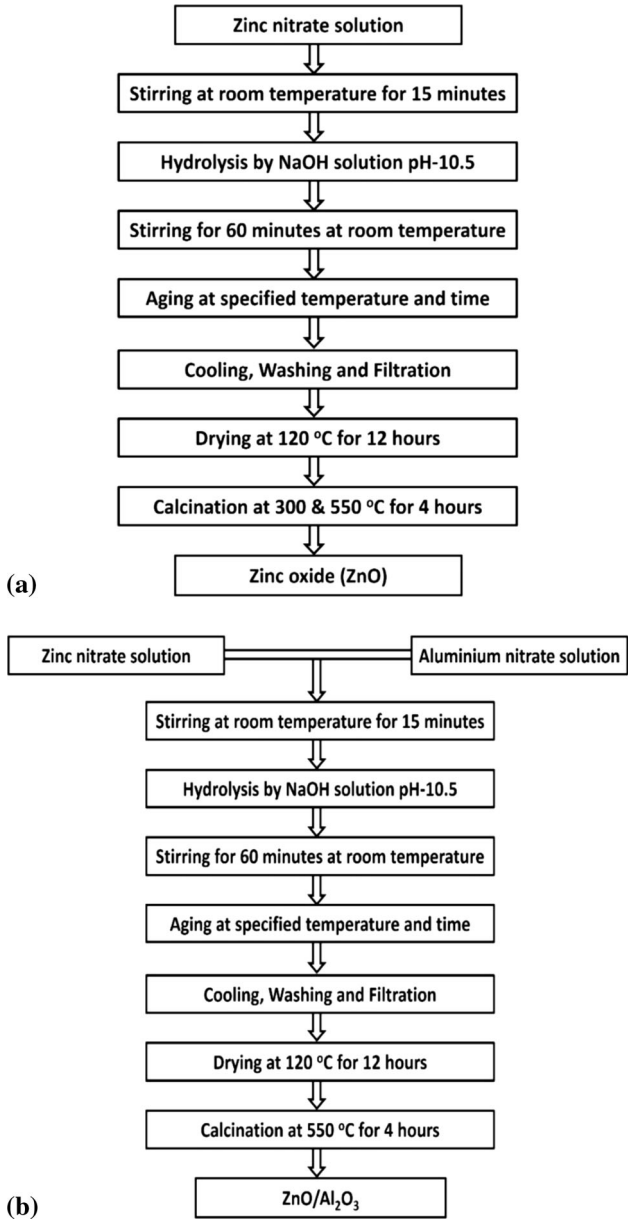

Fig. 1 Preparation steps for (a) bulk zinc oxide at different calcination temperatures and (b) supported zinc oxide adsorbent

2.4 Desulfurization Experiment

The experimental setup used for gas phase removal of thiophene is shown in Fig. 2. The solution of thiophene in toluene (2000 ppm) was taken in a three-neck round bottom flask. Hydrogen was passed through the flask at flow rate of 90 ml/min, which carried the thiophene vapor to the adsorbent bed. The corresponding initial vapor phase concentration of thiophene was about 200 ± 10 ppm. Adsorption was carried out in down-flow packed bad reactor. For each test, 0.25 gm of adsorbent was mixed with 1 gm of quartz. The adsorbent bed height was about 10 mm. Thiophene concentrations were measured at inlet and outlet of absorber using GC (Bruker 450-MS) equipped with PFPD detector. Adsorbents were reduced in situ in flow of mixture of H_2/N_2 flow (30/40 ml/min) for 1 h at 400-475 °C prior to the test followed by cooling to room temperature in nitrogen.

3. Results and Discussion

3.1 Surface Area and Pore Size Analysis

N_2 adsorption–desorption isotherms of all adsorbents are shown in Fig. 3(a). For all samples, the isotherms were of type II with H3 hysteresis loop corresponding to slit shape wide pores (Ref 21). The nitrogen adsorption decreased with the increase in calcination temperature from 300 to 550 °C for bulk zinc oxide adsorbents. Accordingly, with the increase in calcination temperature the BET surface area as well as the total pore volume of zinc oxide decreased sharply as shown in Table 1. The ZnO-300 sample has the surface area of 30.5 m^2/g and the pore volume of 0.181 ml/g which decreased to 14.6 m^2/g and 0.08 ml/g, respectively, for ZnO-550 sample. With the increase in the calcination temperature, the decrease in surface area and pore volume of zinc oxide sample can be attributed to sintering. The surface area and pore volume were higher for supported $30ZnO/Al_2O_3$-550 compared to that of bulk zinc oxide adsorbents which can be attributed to the presence of high surface area alumina (Table 1). Micropores were not observed for any sample.

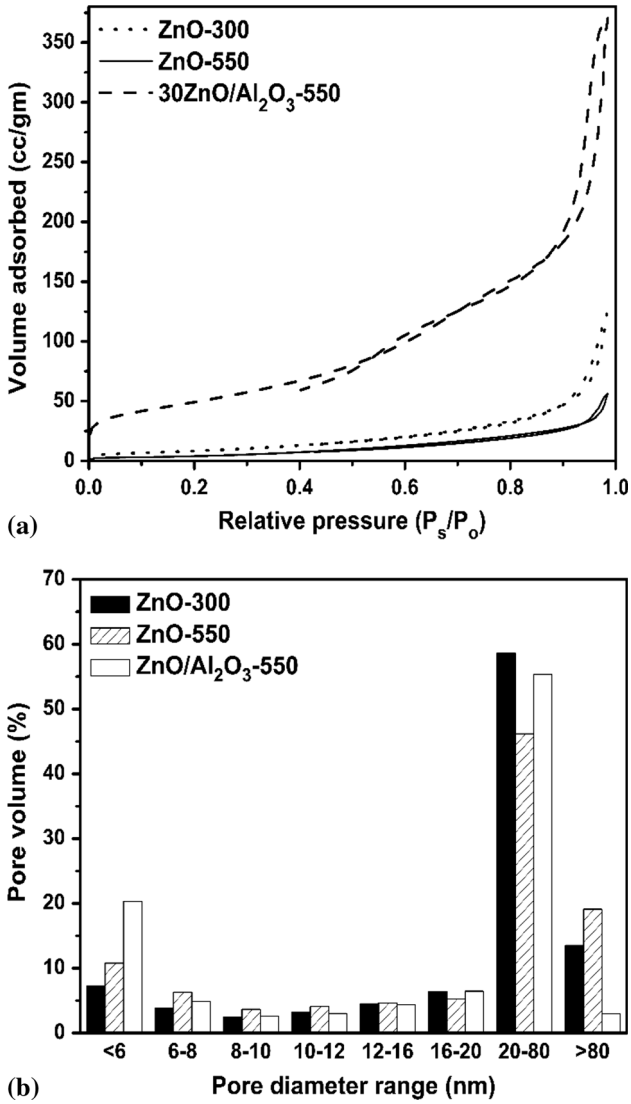

Fig. 3 (a) N_2 adsorption–desorption isotherms, (b) pore size distribution of bulk and supported zinc oxide-based adsorbents

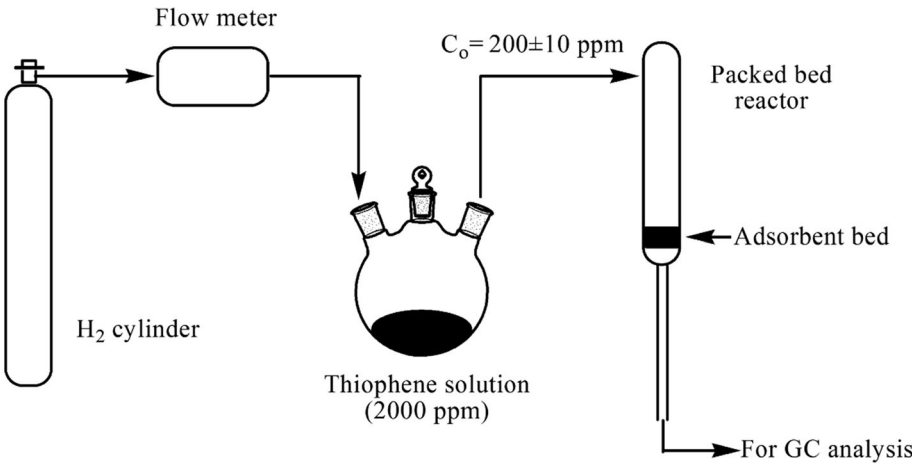

Fig. 2 Schematic diagram of experimental setup for gas phase thiophene removal

Table 1 BET surface area, pore volume and average pore size of adsorbents

Sample ID	Surface area, m^2/g	Total pore volume, ml/g	Average pore size, nm
ZnO-300	30.5	0.18	42
ZnO-550	14.6	0.08	45
Alumina (Al_2O_3)	239	0.45	8
30ZnO/Al_2O_3-550	177	0.55	27
ZnO-550 (used)	13.8	0.14	54
30ZnO/Al_2O_3-550 (used)	125	0.25	32

The micropore area was zero for all samples

The pore size distributions of bulk and supported zinc oxide adsorbents are shown in Fig. 3(b). For bulk zinc oxide-based adsorbents, majority of the pores (46-58%) were in large mesopore and macropores region of 20-80 nm and 13-19% were macropores having size over 80 nm. On increasing calcination temperature from 300 to 550 °C, pores in the range of 20-80 nm decreased with simultaneous increase in volume percentage pores in the range of 2-16 nm and macropores above 80 nm. This can be attributed to partial collapse of the pore structure and accordingly the average pore size (Table 1) of the adsorbent, increased with calcination temperature. The adsorbent 30ZnO/Al_2O_3-550 showed similar pore size distribution pattern as that of bulk zinc oxide, with significant amount of large mesopore and macropore in the region 20-80 nm. The highest average pore diameter of 45 nm was observed for ZnO-550.

3.2 XRD Analysis

Figure 4 shows the XRD patterns of the bulk and supported zinc oxide-based adsorbents. For the bulk adsorbents, the peaks were obtained at 2θ = 31.7°, 34.4°, 36.2°, 47.5°, 56.6°, 62.8°, 67.9°, 69.1° corresponding to hexagonal structure of zinc oxide (JCPDF file no. 00-036-1451). It was observed that with the increase in the calcination temperature from 300 to 550 °C, the intensity of peaks increased suggesting higher crystallinity for ZnO-550 adsorbent. In case of 30ZnO/Al_2O_3-550 adsorbent, the peaks for γ-alumina were observed at 2θ = 37.3°, 45.1°, 66.3° (Ref 22), peaks for cubic $ZnAl_2O_4$ observed at 2θ = 60° (JCPDF file no.01- 073-1961) and that for hexagonal ZnO at 2θ = 31.7°, 36.2° (JCPDF file no. 00-036-1451). The intensity of ZnO peaks in 30ZnO/Al_2O_3-550 adsorbent was much lower as compared to that of bulk zinc oxide adsorbents due to lower content of zinc oxide in the former. Based on the highest intensity peak of zinc oxide (2θ = 36.2°), the average crystallite size was estimated by the Debye–Scherrer equation for all samples. The average crystallite size of zinc oxides calcined at 300 and 550 °C was 41 and 55 nm, respectively, suggesting increase in ordered structure with increase in calcination temperature. The average ZnO crystallite size for supported adsorbent (30ZnO/Al_2O_3-500) was 12 nm, suggesting the metal to be in dispersed state on alumina support.

3.3 TPR Analysis

The TPR profiles of the bulk and supported zinc oxide-based adsorbents are shown in Fig. 5. TPR analysis of the different samples was done to study the reducibility of zinc

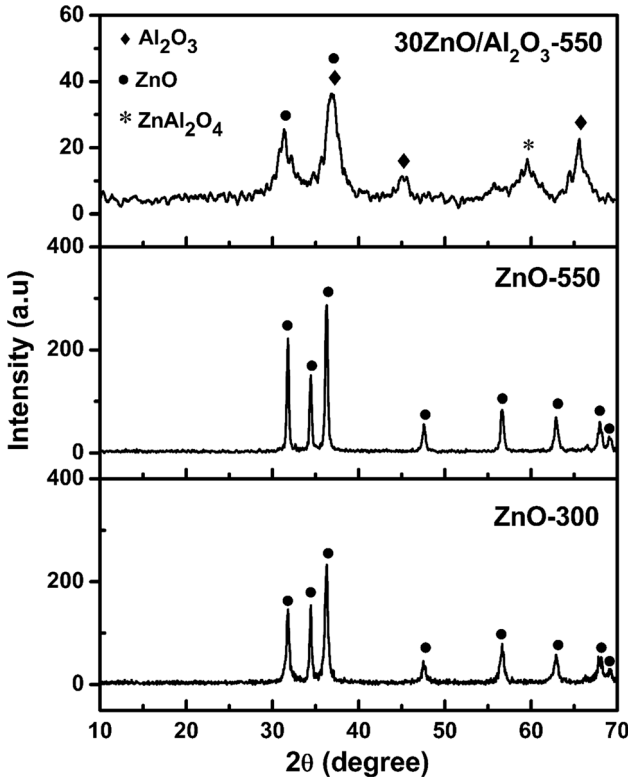

Fig. 4 XRD patterns of bulk and supported zinc oxide-based adsorbents

oxide in various forms. It is well known that higher reduction temperature of metal oxide in TPR profile corresponds to difficulty in reducibility of the oxide and vice versa. Difficulty in reducibility is further associated with the lower activity (Ref 23). The main reduction peaks for ZnO-300 and ZnO-550 adsorbents were observed at 625 and 475 °C, respectively, suggesting latter to be more easily reducible and hence more active. Higher average pore size and crystallite size for ZnO-550 sample compared to that of the ZnO-300 may have facilitated hydrogen diffusion and reduction reaction contributing to higher reducibility. For supported adsorbent 30ZnO/Al_2O_3-550, two main peaks were observed at 425 and 555 °C. The intensity of these peaks was very low than that of the bulk zinc oxide adsorbents, which may be attributed to the presence of lower amount of zinc oxide in the support. The appearance of two reduction peaks suggested two types of metal species on

support. The amount of species less easily reducible was more as indicated by higher area under the peak at 555 °C. Higher interaction between zinc oxide and the alumina as well as lower diffusion of hydrogen (due to lower average pore size) might have contributed to lower reducibility.

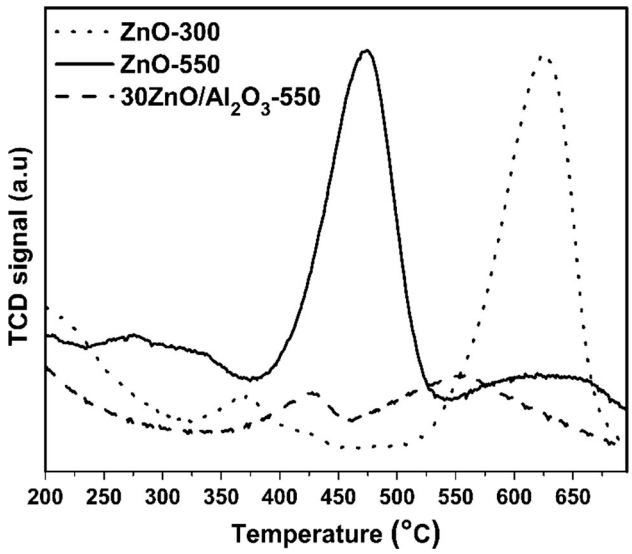

Fig. 5 TPR profiles of bulk and supported zinc oxide-based adsorbents

3.4 FESEM Analysis

The morphologies of various bulk and supported zinc oxide adsorbents are shown in Fig. 6. Distinctive changes in the morphology of the zinc oxide were observed with the preparation methods. Uniform porous structure was obtained for ZnO-300 and ZnO-550. At higher calcination temperature, pore size can be observed to increase, as was also deduced from pore analysis, reported in Table 1. The $30ZnO/Al_2O_3$-550 adsorbent showed a more agglomerated morphology corresponding to that of alumina support.

3.5 Desulfurization Performance over Bulk and Supported Zinc Oxide Adsorbents

Figure 7(a) shows the breakthrough curve for the removal of thiophene at room temperature using hydrogen as carrier gas. The removal of thiophene was most significant for ZnO-550. The ZnO-300 and $30ZnO/Al_2O_3$-550 were both saturated after 120 min of process time. At the same process time of 120 min, ZnO-400 and ZnO-550 were only 80 and 50% saturated, respectively. Thus, ZnO-550 adsorbent showed the highest activity for removal of thiophene. This was in spite of lowest surface area. For thiophene adsorption on bulk zinc oxide-based adsorbents, accessibility to active sites might have been more important as available sites were abundant. The higher removal efficiency for the ZnO-550 in spite of lower surface area and total pore volume may be attributed to its higher average pore size and higher percentage of larger pores. This enhanced accessibility to the interior of the adsorbent for large thiophene molecules,

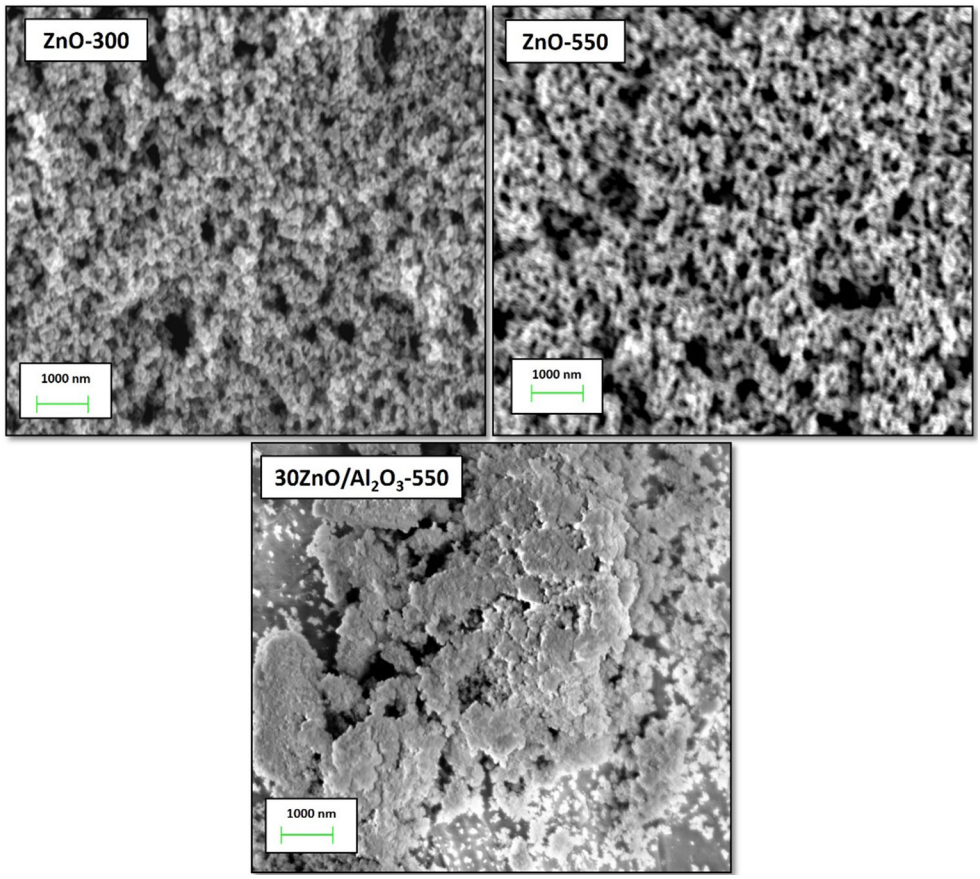

Fig. 6 FESEM images of bulk and supported zinc oxide-based adsorbents

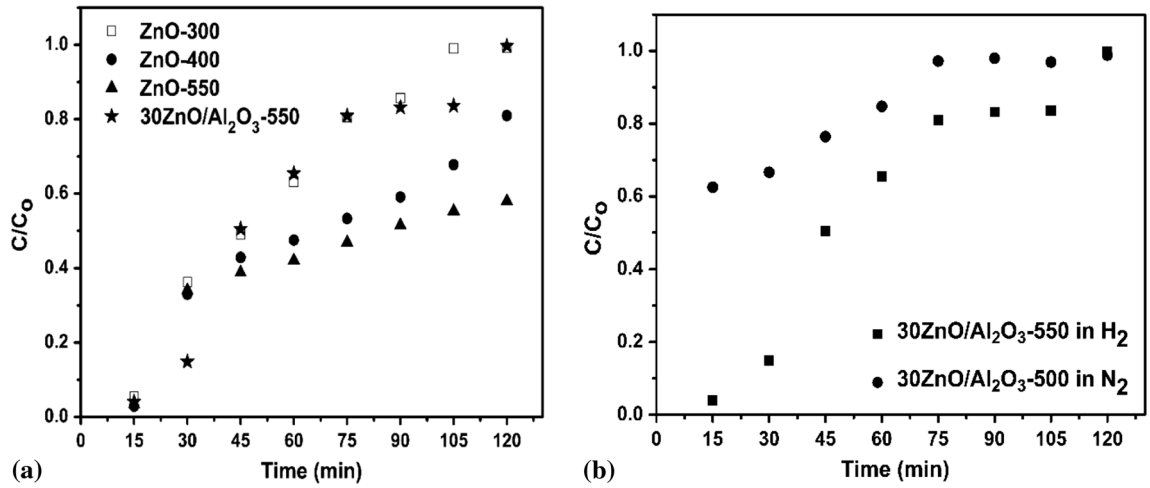

Fig. 7 Desulfurization breakthrough curves of (a) bulk and supported zinc oxide-based adsorbents, (b) effect of carrier gas (H_2/N_2) for supported zinc oxide adsorbent

particularly at the latter stage of adsorption. Consequently for ZnO-550, adsorption continued long after other adsorbents were saturated. There was not much difference in thiophene removal efficiency for ZnO-300 and $30ZnO/Al_2O_3$-550 adsorbents. However, thiophene removal efficiency of ZnO-400 was better than that of both ZnO-300 and $30ZnO/Al_2O_3$-550 adsorbents.

3.6 Desulfurization Performance in the Presence of Different Carrier Gas

The effect of carrier gas on sulfur removal efficiency was studied using supported adsorbent. Adsorption was carried out using hydrogen or nitrogen carrier gas over $30ZnO/Al_2O_3$-550 adsorbent, and results are shown in Fig. 7(b). It was observed that, with change in carrier gas, the initial gas phase concentration changed. For nitrogen as a carrier gas, the initial gas phase concentration was 83 ± 10 ppm and that in hydrogen was 200 ± 10 ppm. Significantly higher sulfur compound removal efficiency was observed when hydrogen was used as the carrier gas compared to that of the nitrogen. For nitrogen, 40% removal was observed in first 15 min and bed was saturated after 75 min. In hydrogen, in first 15 min the removal of thiophene was 95% and bed was saturated only after 120 min of process time. The higher initial concentration of thiophene in hydrogen carrier gas suggested occurrence of some interaction between thiophene and hydrogen even at room temperature. The presence of hydrogen seemed to also have facilitated the adsorption process. The reactive adsorption in the presence of hydrogen has been reported to facilitate removal of sulfur compounds at higher temperature (Ref 24). The present study showed that even at room temperature the hydrogen has a positive effect on removal of sulfur compound.

3.7 Analysis of Used Adsorbents

Few adsorbents used for desulfurization were analyzed after completion of the experiment for better understanding of the process. Figure 8(a) compares the pore size distributions of fresh and used bulk ZnO-550 and supported ZnO adsorbents. The desulfurization resulted in the decrease in pore volumes in the range of 2-20 nm from 34 to 20% with simultaneous increase in pores from 46 to 56% in the range of 20-80 nm for bulk ZnO-550 adsorbent. This phenomenon suggested blockage of small pores

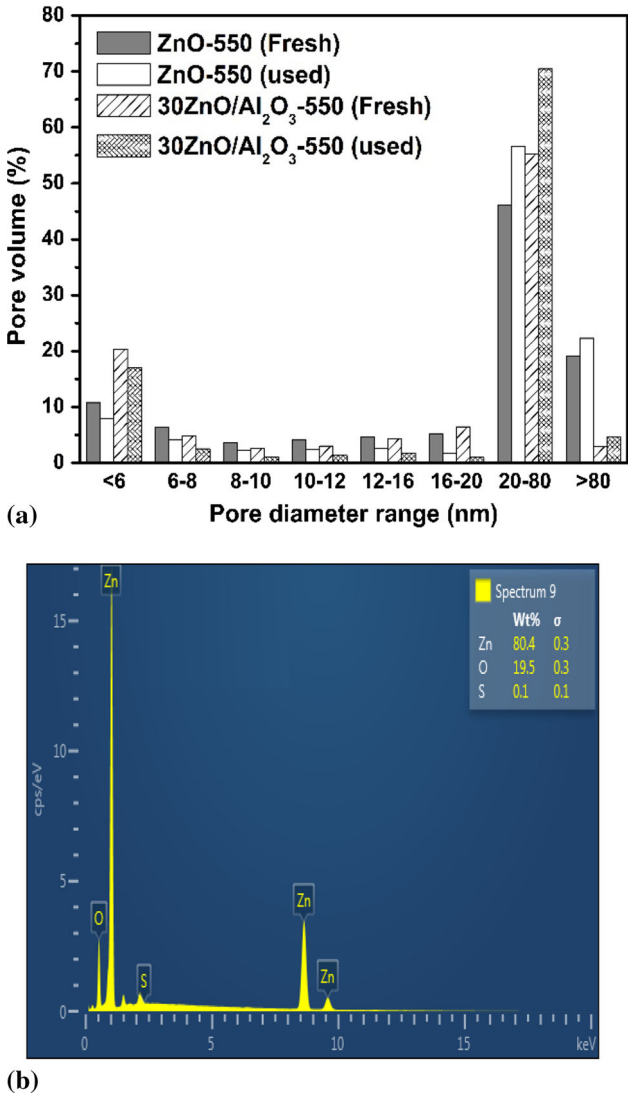

Fig. 8 (a) Pore size distribution of fresh and used bulk ZnO-550 and supported ZnO adsorbents, (b) EDX spectra of used ZnO-550 adsorbent

by sulfur compound, thereby increasing percentage of larger pores in 20-80 nm range and average pore size of the used adsorbent (Table 1). Similar results were also observed for supported ZnO adsorbent. The decrease in pore volumes was from 41 to 25% in the range of 2-20 nm with simultaneous increase to 79 from 59% in the range of 20-80 nm for supported ZnO adsorbent. The surface area of the bulk ZnO-550 adsorbent was observed not to be affected significantly by desulfurization, but that of supported adsorbent was reduced significantly (Table 1). The drastic reduction for the latter may have been associated with the presence of higher percentage of smaller pores in the supported adsorbent. During desulfurization, these smaller pores, which contributed to higher surface area, were blocked extensively, thereby reducing the surface area significantly. The presence of sulfur in used adsorbent was confirmed by the EDX spectrum of used ZnO-550 adsorbent shown in Fig. 8(b). The detected sulfur was 0.1 wt.%.

4. Conclusions

This study investigated the effect of physical properties of zinc oxide, such as surface area, pore size and dispersion, on adsorptive removal efficiency for thiophene in the presence of different carrier gases. Alumina was used as the support to increase the dispersion of the zinc oxide. ZnO-550 adsorbent showed the highest activity for removal of thiophene. The higher removal efficiency for the ZnO-550 was observed in spite of lower surface area and total pore volume. The lower surface area and pore volume may had resulted from the presence of larger pores. However, the large pores made the interior of the adsorbent more accessible to large thiophene molecules, particularly at the latter stage of adsorption and consequently adsorption continued for ZnO-550 long after other adsorbents were saturated. The study showed that, for adsorption of larger molecules, the pore size was the most controlling factor. It was also observed that even at room temperature the hydrogen facilitated removal efficiency of sulfur compound.

References

1. H. Maldonado, A.J. Stamatis, S.D. Yang, R.T. He, and A.Z. Cannella, New Sorbents for Desulfurization of Diesel Fuels via π Complexation Layered Beds and Regeneration, *Ind. Eng. Chem. Res.*, 2004, **43**, p 769-776
2. C. Song, An Overview of New Approaches to Deep Desulfurization for Ultra-Clean Gasoline Diesel Fuel and Jet Fuel, *Catal. Today*, 2003, **86**, p 211-263
3. C. Song and X. Ma, Adsorptive Desulfurization of Diesel Fuel over a Metal Sulfide-Based Adsorbent, *Div. Fuel Chem.*, 2003, **48**, p 522
4. I.V. Babich and J.A. Moulijn, Science and Technology of Novel Processes for Deep Desulfurization of Oil Refinery Streams, *Fuel*, 2003, **82**, p 607-631
5. P. Baeza, G. Aguila, F. Gracia, and P. Araya, Desulfurization by Adsorption with Copper Supported on Zirconia, *Catal. Commun.*, 2008, **9**, p 751-755
6. E.L. Sughrue, G.P. Khare, B.J. Bertus, M.M. Johnson, Desulfurization and Novel Sorbents for Same, U.S. Patent 6254766, 2001
7. R.T. Yang, *Adsorbents: Fundamentals and Applications*, Wiley, New York, 2003
8. A.J. Hernández-Maldonado and R.T. Yang, Desulfurization of Diesel Fuels via π-Complexation with Nickel (II)-Exchanged X- and Y Zeolites, *Ind. Eng. Chem. Res.*, 2004, **43**, p 1081-1089
9. A. Bösman, L. Datsevich, A. Jess, A. Lauter, C. Schmitz, and P. Wasserscheid, Deep Desulfurization of Diesel Fuel by Extraction with Ionic Liquids, *Chem. Commun.*, 2001, **0**, p 2494-2495. https://doi.org/10.1039/B108411A
10. K. Tawara, T. Nishimura, H. Iwanami, T. Nishimoto, and T. Hasuike, New Hydrodesulfurization Catalyst for Petroleum-Fed Fuel Cell Vehicles and Cogenerations, *Ind. Eng. Chem. Res.*, 2001, **40**, p 2367-2370
11. K. Tawara, T. Nishimura, and H. Iwanami, Ultra-deep Hydrodesulfurization of Kerosene for Fuel Cell System, *Sekiyu Gakkaishi*, 2000, **43**, p 105-113
12. Y. Yang, Y. Zhang, L. Wang, Y. Zhang, Z. Jiang, and C. Li, Ultra Deep Adsorptive Desulfurization of Solvent Oils by Ni/ZnO Adsorbent, *Petrochem. Technol.*, 2008, **37**, p 243-246
13. I. Bezverkhyy, A. Ryzhikov, G. Gadacz, and J.P. Bellat, Kinetics of Thiophene Reactive Adsorption on Ni/SiO_2 and Ni/ZnO, *Catal. Today*, 2008, **130**, p 199-205
14. I. Bezverkhyy, O.V. Safonova, P. Afanasiev, and J.P. Bellat, Reaction Between Thiophene and Ni Nanoparticles Supported on SiO_2 or ZnO In Situ Synchrotron X-Ray Diffraction Study, *J. Phys. Chem. C*, 2009, **113**, p 17064-17069
15. C. Caddeo, G. Malloci, G.M. Rignanese, L. Colombo, and A. Mattoni, Electronic Properties of Hybrid Zinc Oxide-Oligothiophene Nanostructures, *J. Phys. Chem. C*, 2012, **116**, p 8174-8180
16. M. Xue, R. Chitrakar, K. Sakane, T. Hirotsu, K. Ooi, Y. Yoshimura, M. Toba, and Q. Fengb, Preparation of Cerium-Loaded Y-Zeolites for Removal of Organic Sulfur Compounds from Hydrodesulfurized Gasoline and Diesel Oil, *J. Colloid Interface Sci.*, 2006, **298**, p 535-542
17. S.H. Kang, J.W. Bae, H.T. Kim, K.W. Jun, S.-Y. Jeong, and K.V.R. Chary, Effective Removal of Odorants in Gaseous Fuel for the Hydrogen Station Using Hydrodesulfurization and Adsorption, *Energy Fuels*, 2007, **213**, p 537-3540
18. J. Shangguan, Y. Zhao, H. Fan, L. Liang, F. Shen, and M. Miao, Desulfurization Behavior of Zinc Oxide Based Sorbent Modified by the Combination of Al_2O_3 and K_2CO_3, *Fuel*, 2013, **108**, p 80-84
19. P. Dhage, A. Samokhvalov, D. Repala, E.C. Duinc, and B.J. Tatarchuka, Regenerable Fe-Mn ZnO/SiO_2 Sorbents for Room Temperature Removal of H_2S from Fuel Reformates: Performance, Active Sites, Operando Studies, *Phys. Chem. Chem. Phys.*, 2011, **13**, p 2179-2187
20. T. Jirsak, J. Dvorak, and J.A. Rodriguez, Chemistry of Thiophene on ZnO, S/ZnO, and Cs/ZnO Surfaces: Effects of Cesium on Desulfurization Processes, *J. Phys. Chem. B*, 1999, **103**, p 5550-5559
21. K.S.W. Sing, D.H. Everett, R.A.W. Haul, L. Moscou, R.A. Pierotti, J. Rouquerol, and T. Siemieniewska, Reporting Physisorption Data for Gas/Solid Systems with Special Reference to the Determination of Surface Area and Porosity, *Pure Appl. Chem.*, 1985, **57**, p 603-619
22. S. Rane, O. Borg, J. Yang, E. Rytter, and A. Holmen, Effect of Alumina Phases on Hydrocarbon Selectivity in Fischer–Tropsch Synthesis, *Appl. Catal. A*, 2010, **388**, p 160-167
23. K. Ebitani and H. Hattori, Combined Temperature-Programmed Reduction (TPR)-Temperature-Programmed Desorption (TPD) Study of Supported Platinum Catalysts, *Bull. Chem. Soc. Jpn.*, 1991, **64**, p 2422-2427
24. A. Ryzhikov, I. Bezverkhyy, and J.P. Bellat, Reactive Adsorption of Thiophene on Ni/ZnO: Role of Hydrogen Pretreatment and Nature of the Rate Determining Step, *Appl. Catal. B Environ.*, 2008, **84**, p 766-772